Asian Journal of Chemistry; Vol. 25, No. 14 (2013), 8136-8140

ASIAN JOURNAL OF CHEMISTRY

http://dx.doi.org/10.14233/ajchem.2013.15271

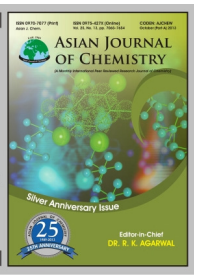

Synthesis of Porous Carbon Materials by the Replication of Organoclays

NGUYEN TIEN THAO* and PHAM THI HIEN

Faculty of Chemistry, VNU University of Science, 19 Le Thanh Tong, Hanoi, Vietnam

*Corresponding author: Fax: +84 4 38241140; Tel: +84 4 39331605; E-mail: ntthao@vnu.edu.vn

(*Received*: 4 February 2013; *Accepted*: 5 August 2013) AJC-13890

Di Linh (Vietnam) clay was chemically treated and modified by cetyltrimethylammonium bromide to prepare the organoclays with high interlayer spacings. The organoclay samples are further used as the hard template for the synthesis of porous carbon materials. The removal of clay template yield porous carbon materials having a moderate surface area (80-290 m^2/g), micro- and mesoporous structure. The morphology of the carbon products is well correlated with the characteristic properties of clay templates. The unpillared clays lead to the formation of carbon nanoparticles with rather high large surface area and more porosity while organoclays gives carbon nanosheets and the medium specific surface area.

Key Words: Porous carbon, Hard template, Cetyltrimethylammonium bromide, Nanoparticle, Nanosheets.

INTRODUCTION

Porous carbon materials are widely characterized by their highly developed internal and external surface area and porosity as well. They possess both micro- and mesopores which play an important role in the absorption of large amounts of various chemicals from gases or liquids[1,2].

Based on these valuable features, porous carbon materials are used extensively as electrode materials for batteries, fuel cells and as sorbents for separation processes[3,4], as supports for many important catalytic processes[1,5]. Their use in such diverse applications is known as the results of their superior physical and chemical properties (electric conductivity, thermal conductivity, chemical stability, low density, *etc*.) and their wide availability as well[4]. Thus, many advances have been made for the improvement of fabrication methods and the development of new synthetic techniques as well[3,5-7]. One of the great efforts relating to the synthetic methods is called a hard-template synthesis[6,8,9]. In this way, the templates mainly serve as structural molds for the negative replication of mesoporous carbon materials and no significant chemical interaction occurs between inorganic template components and carbon precursor. The corresponding replicated carbon structures are predetermined by the textural templates, which usually lead to the formation of well-defined nanostructural products[9,10]. Many inorganic templates have been used to synthesize a wide variety of carbon materials. For instance, alumina[10], silica[11], mesoporous silica[12,13] have been used as templates to produce microporous carbonaceous materials and carbon nanotubes/nanowires. In addition, several layered materials as double hydroxides and clays[14], sepiolite[15], bentolite[16,17] or microporous zeolites[17,18] were also used as selected molds to produce nanoporous carbon materials. The objective of this present contribution is to report the synthesis of nanoporous carbon materials used typically modified organoclays as the templates.

EXPERIMENTAL

Organoclay template and porous carbon preparation: Di Linh clay mineral (Di Linh, Lam Dong Province, Vietnam) was supplied by Drilling Mud Joint Stock Corporation, Vietnam. Firstly, 15 g of the clay was washed several times with distilled water prior to the addition of HCl 0.5 M solution with continuous stirring for 24 h. The suspension was filtered, washed with deionized water and dried in an oven at 40 ºC. The obtained solid was further treated with 0.5 M sodium chloride solution at room temperature for 24 h. The resultant was filtered, washed and then dried at 110 ºC. Secondly, CTAB-montmorillonite was synthesized typically as follows: quantity of 10.0 g of treated clay was carefully mixed with 5 g of solvent. Then a desired amount of cetyltrimethyl ammonium bromide (CTAB) was added in good mechanical stirring to obtain the slurry. The resultant was then evaporated at 90-130 ºC.

Four Di Linh CTAB-pillared clays with different interlayer spacings were used as hard-templates for the synthesis of templated carbons. Typically, 5 g of pre-dried CTAB-pillared clay was mixed with 2 mL of a solution containing 1.5 g of

glucose and 0.22 g of H_2SO_4 at room temperature. The slurry was then dried at 100 ºC for 6 h before heating to 160 ºC for 6 h (10 ºC/min) in air. This process was repeated three times to enhance the amount of glucose inserting between interlayer spaces of the template. Then, the obtained glucose/clay solid was carbonized in a flow of 50 mL/min of Ar at 700 ºC for 6 h at a ramp of 5 ºC/min. The inorganic component was subsequently removed using a 20 wt % NaOH/H_2O-EtOH solution (v:v = 50:50) three times. It was assumed that the tetrahedral/octahedral layers were dissolved during these treatments. The carbonized solid was further washed by 0.5 M HCl three times in order to remove unleached metal oxides prior to drying in an oven at 80 ºC overnight. The final back carbon powder was respectively designated as NC- symbols. For the case of NC-4, the hard template was prepared from an organoclay (37.5 wt % CTAB) fully extracted cetyltrimethyl ammonium bromide pillars by ethanol solvent prior to the impregnation of glucose solution.

Characterization: The elemental composition of raw clay and final product impurities was also measured using an AA-6800 atomic absorption spectrophotometer (Shimadzu, Japan). X-ray diffraction spectra of synthesized carbons were collected on a D8ADVACE diffractometer with CuK_α (l = 1.54056 Å) radiation operating 40 mA. The scanning range was from 4000-400 cm^{-1} with a resolution of 4 cm^{-1}. The scanning electron microscopy (SEM) microphotographs were obtained in a JEOS JSM-5410 LV. Nitrogen adsorption isotherms were measured at -196 ºC on a Gemini VII 2390 V1.02 apparatus from Quantachrom Corporation, after having degassed the sample under vacuum at 150 ºC. Energy-dispersive spectroscopy (EDS) data were obtained from Varian Vista Ax X-ray energy-dispersive spectroscope.

RESULTS AND DISCUSSION

Chemical composition and X-ray diffraction: Di Linh clay was chemically pretreated to remove contaminants and its chemical composition was indicated in Table-1. The basal spacing of CTAB-intercalated clays was determined by X-ray diffraction. Fig. 1 shows XRD patterns of Di Linh clay pillared by different amounts of cetyltrimethyl ammonium bromide. Firstly, all layered clays exhibit strong reflection peaks around 2θ of 3.5; 6.8; 17.4; 21.6; 24.4; 26.8; 31.8 characterizing the

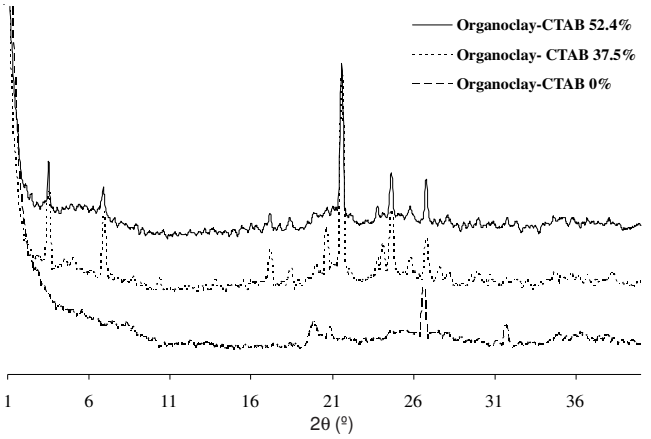

Fig. 1. XRD patterns of organoclay templates

presence of montmorillonite phases[19-21]. The interlayer distance of silicate layers are in the range of 1.4-2.6 nm[21], corroborated by the appearance of the reflection peak at 2 theta values of 3.48º (Fig. 1).

Table-2 indicates that the clay gallery varies with the CTAB/clay ratio[20]. The interlayer distances reach a maximal value as the amount of CTAB inserting at 37.5 wt. % (Table-2). At a higher CTAB amount, the basal spacing of clay templates slightly decreases[21]. This is believed to correlate with the geometry of the CATB micelle[19]. The average radius of a spherical CTAB micelles is known to be *ca.* 13 Å while the interlayer distance in the treated clay is approximately 15.3 Å (Table-1). Thus, under typical experimental conditions, spherical CTAB micelles were intercalated into clay interlayers resulting in an observable expansion of clay gallery[19] (Table-2). As a result, the thicker carbon films may obtain as these organoclays are used as structural molds for the production of carbon materials[22]. After carbonizing carbohydrates followed by removal of the inorganic template, the final carbon products were recorded X-ray diffraction at both small and large angles (Figs. 2 and 3). As seen in Fig. 2, all clay templated carbon materials show no 2θ reflection angles matched with those for organoclays as compared with Fig. 1. Instead, these patterns appear a broad peak around 26º and a low intensity signal at 44º charactering the formation of carbonaceous materials[2,16]. Moreover, no reflection signals appear at small reflection angles (Fig. 3), reflecting the successful removal of clay

TABLE-1
CHEMICAL COMPOSITION OF MINERAL AND THE CHEMICAL TREATED CLAY

Sample	Chemical composition (wt.%)							
	SiO_2	Al_2O_3	Fe_2O_3	TiO_2	CaO	MgO	Na_2O	Others
Mineral	51.5	16.7	7.0	4.82	0.78	2.83	0.54	15.83
Treated clay	54.2	18.8	9.7	6.26	0.98	1.88	1.39	6.79

TABLE-2
CHARACTERISTICS OF ORGANOCLAY TEMPLATED-CARBON MATERIALS

Batch No.	Organoclay templates			Templated carbon product			
	CTAB (wt.%)	d_{001} (Å)	BET surface (m^2/g)	Product named	Micropore area (m^2/g)	External area (m^2/g)	BET surface area (m^2/g)
1	0	15.53	147.0	NC-1	183.9	88.7	272.8
2	37.5	26.20	31.5	NC-2	76.6	108.7	185.3
3	52.4	25.17	23.7	NC-3	25.9	55.8	81.2
4	–	16.50	17.3	NC-4	135.7	152.8	288.5

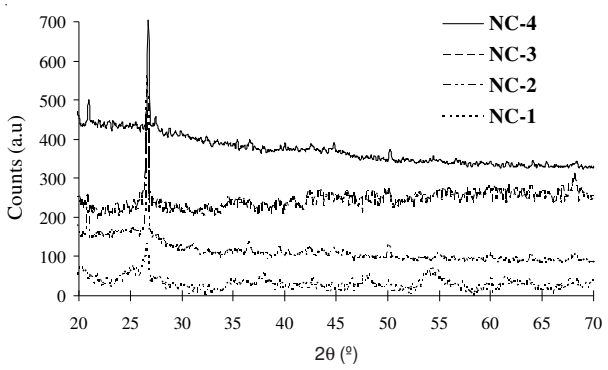

Fig. 2. XRD patterns at large 2θ of 20-70º for organoclay templated carbon materials

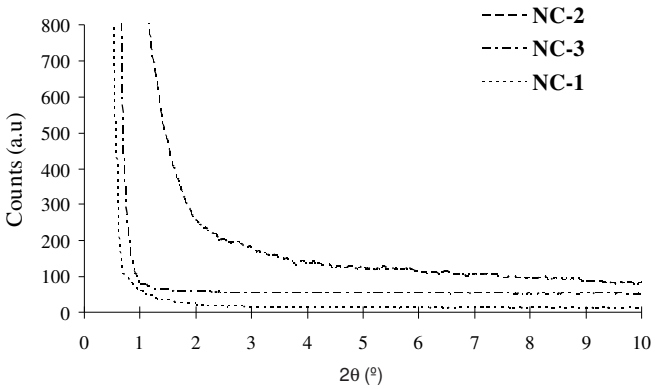

Fig. 3. XRD patterns at low 2θ of 1-10º for organoclay templated carbon materials

templates. The absence of the small angles also reveals that the final carbon product was not well inherited the ordered layered structures from their organoclay templates. Indeed, the micellar surfactant pillars are gradually vanished during the pyrolysis process, leading to the formation of disordered carbon nanosheets after leaching the inorganic framework[6,17].

SEM and TEM: The morphology of both clay templates and final produced carbon materials were investigated by SEM and TEM techniques. Microscopic examination indicates a remarkable morphological resemblance between templates and fabricated carbon materials, in good accordance with the results reported in literature[2,6,11,13,15,18,20,22]. The SEM photographs of montmorillonite templates only (0 % and extracted CTAB sample) display the sphere-like grains of the clay minerals. The clay platelets are stacked together and form agglomerates[18]. In various areas, it is observed a compactness of clay particles to make micrometric slabs (Fig. 4A) and nanorods (Fig. 4G). As intercalated by CTAB, physical appearance of the clay particles has significantly changed. The sphere-like particles were replaced by irregularly-shaped pellets[20]. In various parts of the SEM photographs of these organoclays, the grain boundaries appear wavy lattice fringes, revealing the existence of layered structure. These changes in the morphologies and particle shape confirm the intercalation accompanied by adsorption of surfactant species. Furthermore, an increased loading amount of CTAB gives rise to the organoclay surface becomes smoother (Fig. 4C and 4E).

The photographs of NC-1 and NC-4 shown in Fig. 4B and 4H appear well-defined nanoparticles[17]. TEM results also

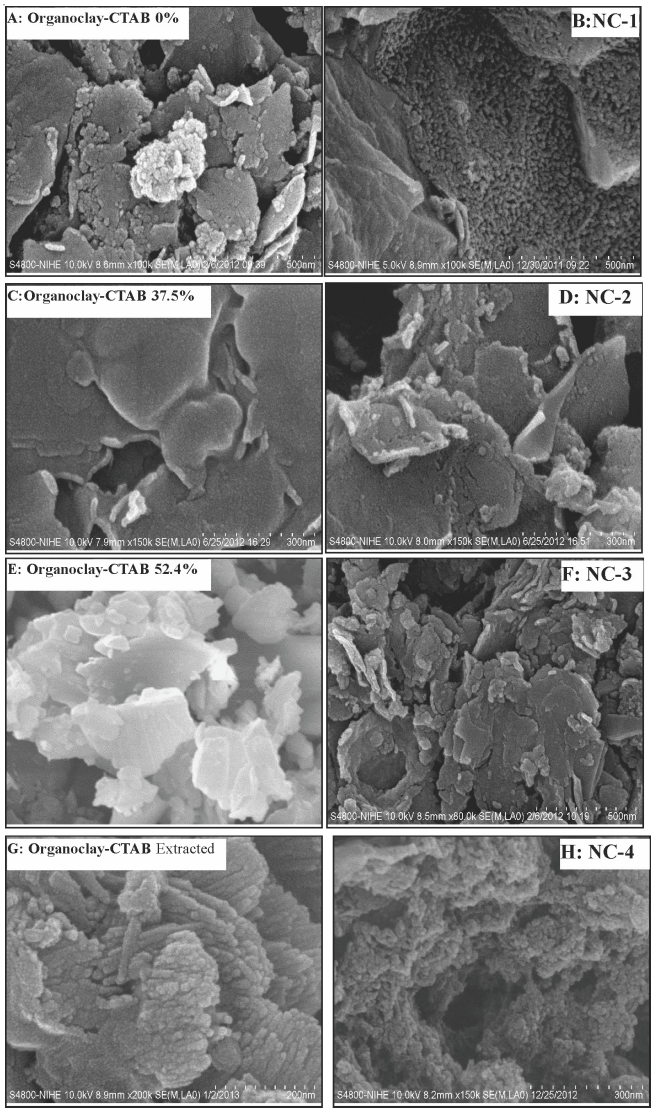

Fig. 4. SEM images of organoclays (left) and the final carbon materials (right)

confirm the analogous morphology between the clay templates and their derived-carbon products. As seen in Fig. 5, NC-1 sample is composed of numerous uniformly spherical carbon nanoparticles with the diameter in the range of 20-30 nm (Fig. 5). There are a lot of voids between the nanosheets that may build up to the slit-shaped spaces[23]. This observation is further supported by the conclusions drawn from nitrogen sorption analysis below.

In a similar way, NC-2 and NC-3 carbon samples also show the similar topographical feature to their organoclay templates. Fig. 4D indicates that NC-2 is consisted of folded thickness nanosheets while NC-3 (Fig. 4F) comprises numerous carbon nanoslabs. The TEM images of samples NC-2 and NC-3 in Fig. 5 illustrate the large carbon nanosheets piled disorderly on each other[17] while those of their organoclay templates present the dark lines in parallel, corresponding to the individual silicate layers[21,23]. As the interlayer spaces are well filled with carbon precursor; the polymerization of carbohydrate leads to the formation of exfoliating nanocomposite. The removal of silicate component in such a nanocomposite yields the random arrangement of negatively replicated carbon layers.

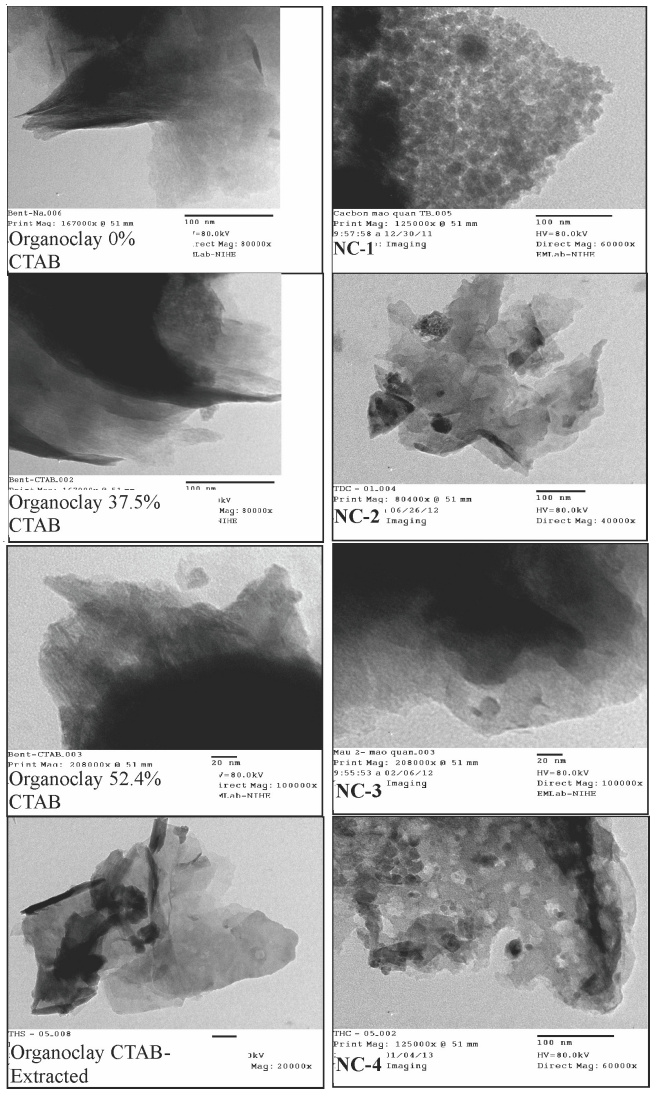

Fig. 5. TEM images of the two CTAB-Di Linh-clay templated carbons

The carbon sheets are hundred nanometers in both length and width, but just a few nanometers in thickness that corresponds to the basal spacing of organoclays[17,19]. The disordered arrangement of carbon sheets yields a porous structure of the final carbonaceous products.

Nitrogen physical absorption: Analysis of nitrogen adsorption isotherms brings more useful information about the porosity of all samples. Table-2 also collected the BET surface area and micropore area which is estimated from t-plot. As indicated in Fig. 6, nitrogen adsorption isotherms for NC-2 and NC-3 do not present a plateau exactly parallel to the relative pressure axis, they presents a thin hysteresis loop, representing the occurrence of adsorption in some kind of mesoporosity in addition to that in micropores[17]. In particular, their hysteresis loops do not close even at P/P_o of 0.1 which could characterize instability of the pore systems[16,23]. Unlike the nitrogen adsorption/desorption curve(s) for NC-2(3), the isotherms for NC-1 and NC-4 clearly appear a broad hysteresis loop which strongly indicates the presence of mesopores in such materials. These latter carbon samples have a H2 hysteresis loop which characterizes for open capillaries of complex shapes, pores with narrow and wide section[26], whiles NC-2 and NC-3 exhibit a type H4 hysteresis loop, representing

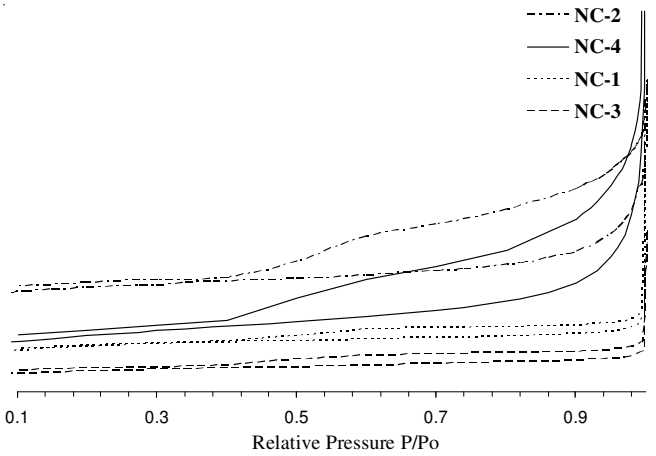

Fig. 6. Nitrogen isotherms of clay templated carbon samples (NC-1 to NC-4

for the aggregates forming the slit-like pores with uniform sizes[22,23]. A significant difference in the nitrogen adsorption isotherms for the final carbon products arises from the negative replication of two different textural clay templates. Samples (NC-1 and NC-4) obtained by carbonization of glucose within the montmorillonite interlayer space without organic pillars and the small voids between fine nanoparticles have similar sorption characteristics (Table-2). The surface areas of such carbon products are rather high with the micropores occupying *ca.* 50-70 % of the total surface area (Table-2). In context, the rest mesopore area are ascribed as the nitrogen adsorption in many slit-shaped capillaries formed between small carbon particles and/or carbon nanosheets[20] (Figs. 4 and 5) those are shown in Fig. 7. On other hand, micropores are formed by the negative replication of imperfection of clay structures and the defects in the carbon product particles after treated in HCl solution. The presence of inorganic impurities in the original clay leads to the formation of a microporous system[9,12] after treating the final solid products in an acidic condition. Therefore, taking account into pore size distribution would elucidate the porosity properties of the carbon materials.

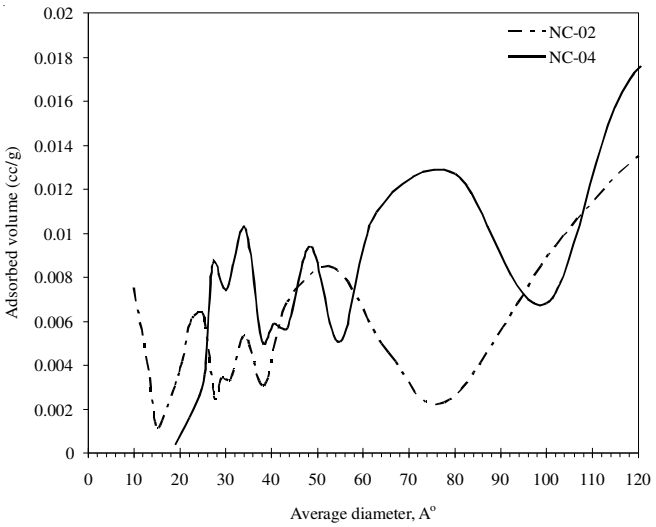

Fig. 7. Pore size distribution (PSD) of sample NC-2 and NC-4

Fig. 7 displays that pore size distribution (PSD) curve for NC-2 sample has a set of peaks at 2.3, 3.4; 5.4 nm and other

broad peak ranged from 5 to 10 nm while that for NC-4 appears at 2.7, 3.4 nm and a wide peak centered at 4.8 nm. Unfortunately, we were unable to estimate the pore size distribution data lower than 1.5 nm in our nitrogen adsorption experiment. In the range of 20-120 Å, a small difference in PSD between two representative carbon samples is observed. The PSD of NC-4 is narrower and more intensive because of the different inorganic templates used. The clay nanoparticles are acting as template to generate micro- and mesoporous carbon sample NC-4 sample while layered organoclay is replicated to produce less porous carbon product[18,22]. As the nitrogen uptake, micropore and mesopore volume of NC-4 are much higher than those of NC-2 pattern.

Electron dispersed X-ray spectroscopy: The analysis of the carbon content provides us with additional information about the nature of the clay templated carbons. Energy-dispersive X-ray spectroscopy (EDX) is a useful analytical tool used for the chemical characterization of the sample surface. In order to investigate the elemental surface composition of the synthesized carbon samples, we have collected an electron dispersed X-ray spectrum for a selected sample NC-2. Fig. 8 shows the spectrum and elemental composition of NC-2. EDS analysis indicates that the sample has remarkable amount oxygen in addition a tiny amount of metal ions. It is not surprising as observed more than 20 % of atomic oxygen in the final templated carbon sample. Since the carbon precursor is glucose, the wall of carbon sheets is believed to possess a remarkable amount of OH groups, in harmony with the results on carbonaceous materials prepared through the replica of mesoporous silica templates[6,8,11].

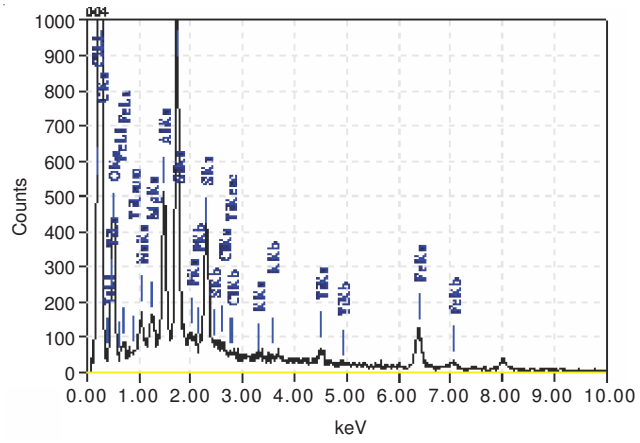

Fig. 8. Energy dispersive X-ray spectrum and surface composition of the clay templated carbon NC-2

The per cent of Na, Mg, Al and Si is very low (< 5 %), in good agreement with the elemental analysis results (not reported here). Therefore the elemental analysis surface strongly substantiated the successful removal of clay template.

Conclusion

The treated Di Linh clay has been pillared by cetyltrimethyl ammonium bromide to increase in d_{001}-spacing of original clay. An intercalation of 37.5 wt.% of CTAB resulted in a remarkably increased interlayer spacing (from 15 to 26 Å) and changes in material morphology. These pillared Di Linh clay was used as a good hard-template candidate for the synthesis of porous carbon material. Four clay templates were impregnated with a glucose solution prior to the carbonization of the glucose/clay composite under inert atmosphere at a high temperature. Unpillared clays were negatively replicated to yield carbon nanoparticles while organoclays act as templates to produce carbon nanosheets. All final carbon samples have both micro- and mesoporous structures and a surface area of 80-290 m^2/g. The porosity of the synthesized carbon samples are made of the arrangement of carbon nanosheets, nanoslabs, nanoparticles and slit-shaped capillaries. The pore size distribution, specific surface area and product morphology is directly dependent on the texture of clay templates. The surface composition of carbon product is consisted mainly of carbon and oxygen component in addition to a tiny amount of unleached Al, Si, Na template. The findings may be a promising route to prepare nanoporous carbon materials through the replication of the pillaring clays.

ACKNOWLEDGEMENTS

This research is funded by Vietnam National University, Hanoi, Asia Research Center under grant number ARC-49/2011/HDDT and QG.12.08.

REFERENCES

1. D. Nguyen-Thanh and T.J. Bandosz, *Micropor. Mesopor. Mater.*, **92**, 47 (2006).
2. P.M. Barata-Rodrigues, T.J. Mays and G.D. Moggridge, *Carbon*, **41**, 2231 (2003).
3. C. Santos, M. Andrade, A.L. Vieira, A. Martins, J. Pires, C. Freire and A.P. Carvalho, *Carbon*, **48**, 4049 (2010).
4. F. Lufrano and P. Staiti, *Int. J. Electrochem. Sci.*, **5**, 903 (2010).
5. J. Garcia-Martinez, T.M. Lancaster and J.Y. Ying, *Adv. Mater.*, **20**, 288 (2008).
6. C. Liang, Z. Li and S. Dai, *Angew. Chem. Int. Ed.*, **47**, 3696 (2008).
7. B. Naik and N.N. Ghos, *Recent Patents Nanotechnol.*, **3**, 213 (2009).
8. H.J. Wu, L.D. Wang, Y.M. Wang, S.L. Guo and Z.Y. Shen, *Mater. Sci. Eng. B*, **177**, 476 (2012).
9. J. Ge, H. Ding and X. Xue, *Angew. Chem. Int. Ed.*, **51**, 6205 (2012).
10. S. Han and T. Hyeon, *Carbon*, **37**, 1645 (1999).
11. S. Jun, S.H. Joo, R. Ryoo, M. Kruk, M. Jaroniec and Z. Liu, *J. Am. Chem. Soc.*, **122**, 10712 (2000).
12. M.F. Lai and J.-K. Kim, *Polymer*, **46**, 4722 (2005).
13. R. Ryong, H.J. Sang and J. Shinae, *J. Phys. Chem. B*, **103**, 7743 (1999).
14. K. Putyera, T.J. Bandosz, J. Jagieo and J.A. Schwarz, *Carbon*, **34**, 1559 (1996).
15. G. Sandi, K.A. Carrado, R.E. Winans, C.S. Johnson and R. Csencsits, *J. Electrochem. Soc.*, **146**, 3644 (1999).
16. G. Sandi, P. Thiyagarajan, K.A. Carrado and R.E. Winans, *Chem. Mater.*, **11**, 235 (1999).
17. C.J. Meyers, S.D. Shah, S.C. Patel, R.M. Sneeringer, C.A. Bessel, N.R. Dollahon, R.A. Leising and E.S. Takeuchi, *J. Phys. Chem. B*, **105**, 2143 (2001).
18. P.M. Barata-Rodrigues, T.J. Mays and G.D. Moggridge, *Carbon*, **41**, 2231 (2003).
19. W.H. Xue, H.P. He, J.X. Zhu and P. Yuan, *Spectrochim. Acta A*, **67**, 1030 (2007).
20. B. Oztop and T. Shahwan, *J. Colloid Interf. Sci.*, **295**, 303 (2006).
21. N. Sarier, E. Onder and S. Ersoy, *Colloid. Surf. A*, **371**, 40 (2010).
22. T. Kyotani, T. Nagai, S. Inoue and A. Tomita, *Chem. Mater.*, **9**, 609 (1997).
23. N. Tien-Thao, M.H. Zahedi-Niaki, HS. Alamdari and S. Kaliaguine, *J. Catal.*, **245**, 348 (2007).